

Essential ocean variables and high value biodiversity areas: Targets for the conservation of marine megafauna



Isabel García-Barón^{a,1,*}, M. Begoña Santos^b, Camilo Saavedra^b, Amaia Astarloa^a, Julio Valeiras^b, Salvador García Barcelona^c, Maite Louzao^a

^a AZTI, Marine Research, Basque Research and Technology Alliance (BRTA), Herrera Kaia Portualdea z/g, Pasaia, Spain

^b Instituto Español de Oceanografía (IEO), Centro Oceanográfico de Vigo, Subida a Radio Faro, 50, 36390 Vigo, Spain

^c Instituto Español de Oceanografía (IEO), Centro Oceanográfico de Málaga, Puerto Pesquero, s/n, 29640 Fuengirola, Málaga, Spain

ARTICLE INFO

Keywords:

Environmental envelope
Biodiversity richness index
Community management
Seabirds
Cetaceans

ABSTRACT

Effective conservation and management measures are needed to face the unprecedented changes that marine ecosystems, and particularly marine megafauna, are suffering. These measures require the identification of high-value biodiversity areas (HVBAs) which in turn require the identification of the essential ocean variables (EOVs) that shape the environmental envelope of communities (*i.e.* space defined by a set of environmental variables). The aim of this study was to delineate and characterise the HVBAs for the north and northwestern Spanish seabird and cetacean community taking advantage of the sightings collected during the annual PELACUS oceanographic survey (2007–2016). We used distance sampling methodology to analyse the species detectability based on environmental conditions. Then, we delimited the HVBAs and identified the EOVs defining the environmental envelope of the community based on a spatio-temporal modelling approach using Generalized Additive Models. Overall, the main environmental variables driving species abundance were the sea surface temperature (SST), the distance to the shelf-break and the chlorophyll-*a* concentration (Chl-*a*). The SST and Chl-*a* were identified as dynamic EOVs due to their highest relative predictor importance, driving the environmental envelope and shaping areas of higher density. HVBAs were located mainly over the northwestern Spanish waters and decreased towards the inner Bay of Biscay remaining spatially stable over the study period. By identifying community-level HVBAs, we can understand the underlying ecological and oceanographic processes driving the spatio-temporal patterns of biological communities, such as those composed by seabirds and cetaceans. This information would identify conservation targets to assist the allocation of management resources. In addition, the location of HVBAs can help to fulfil the emergent need for sound spatial information to support the implementation of marine spatial planning.

1. Introduction

The accelerated loss of biodiversity that marine ecosystems are suffering is a global concern (IPBES, 2019). Human impacts such as overexploitation, pollution and coastal development (Dulvy et al., 2003; Halpern et al., 2008; IPBES, 2019) and also climate change (IPBES, 2019; Simmonds and Smith, 2009; Sydeman et al., 2012) are causing unprecedented changes at global scale. In fact, only 3% of the ocean was described as free from human pressures in 2014 (IPBES, 2019). Among marine fauna, apex predators are particularly vulnerable to human-related threats (Lascelles et al., 2014) due to their life history characteristics and position at the top of the marine food web.

Furthermore, a large proportion of marine megafauna, such as seabirds and cetaceans, seem to have consistent migration pathways (Horton et al., 2017) that difficult their adaptation to bottom-up effects caused by changes in the distribution of their prey (Evans and Bjørge, 2013; Luczak et al., 2011) and/or to shifts in environmental conditions (Macleod, 2009; Soldatini et al., 2016). Therefore, the provision of the spatial patterns of species distribution to identify their essential habitats is a key factor for guiding conservation and management strategies for these species (Evans and Hammond, 2004).

Species-specific oceanographic habitats reflect environmental envelopes (*i.e.* space defined by a set of environmental variables) critical for the species survival resulting from their adaptation to a highly

* Corresponding author.

E-mail address: isa.garciabaron@gmail.com (I. García-Barón).

¹ orcid.org/0000-0001-5962-0819

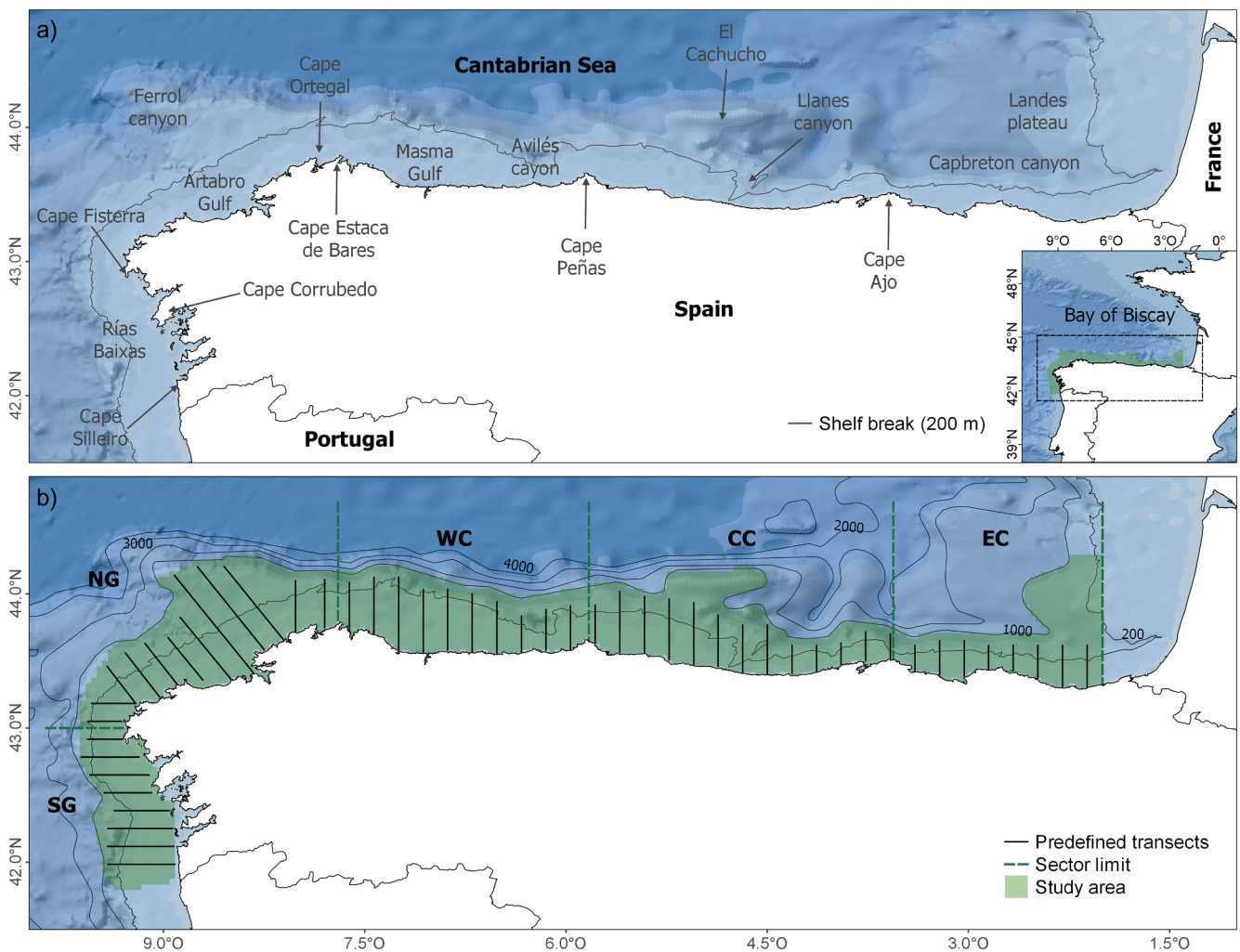


Fig. 1. Map of the study area showing a) the geographic references mentioned in the text; b) the predefined transects followed during the PELACUS oceanographic acoustic surveys (2007–2016) and geographical sectors subdividing the study area: south Galicia (SG), north Galicia (NG), western Cantabrian Sea (WC), central Cantabrian Sea (CC) and eastern Cantabrian Sea (EC) based on Santos et al. (2013).

variable system where feeding resources vary at multiple spatial and temporal scales (Lambert et al., 2018). When information on preyscapes (*i.e.* ecological features describing spatial patterns of prey biomass; Louzao et al., 2019a) of marine megafauna is not available, environmental predictors have been used as proxies of prey distribution. To do this, habitat modelling techniques (*i.e.* species distribution models also known as habitat suitability models or ecological niche models) can be used to identify areas of high probability of presence and/or abundance of individuals by identifying the environmental conditions driving their ecological niche (Holt, 2009; Redfern et al., 2006). Furthermore, habitat modelling techniques can serve to define the environmental conditions or essential ocean variables (EOVs) that shape the environmental envelope of marine megafauna.

Ideally, habitat modelling would be based on accurate presence data at a range of temporal and spatial scales (Redfern et al., 2006). Collecting these data for marine megafauna species requires dedicated surveys over large areas; however, due to the logistics and costs involved, these large scale surveys have been taking place once every 10 years (*e.g.* SCANS surveys, Hammond et al., 2017), leading to few studies showing the consistency of high-value biodiversity areas (HVBAs) over time (*e.g.* Kuletz et al., 2015; McClellan et al., 2014). Thus, the information provided by non-dedicated annual surveys is essential to address habitat preferences over time and can complement the less frequent European dedicated at-sea surveys which are not carried out yearly; *e.g.* SAMM surveys (Laran et al., 2017).

Since 2007, the PELACUS annual oceanographic survey, which is carried out every spring by the Spanish Institute of Oceanography (IEO), collects data on a broad community of seabirds and cetaceans exploiting the coastal and shelf waters of the NW and northern of Spain (Louzao et al., 2019b; Saavedra et al., 2018; Santos et al., 2013). For numerous seabird species, the NW and northern Spanish coast represents a key feeding area during certain periods of the year, when they undertake seasonal feeding migrations into the area (Arcos et al., 2009; Pettex et al. 2017; Astarloa et al., 2019; Louzao et al., 2020a). In the same way, the resource availability and the combination of diverse physiographic characteristics of the environment make these waters a suitable habitat for several species of cetaceans (Lambert et al., 2017a; Laran et al., 2017; Spyraeos et al., 2011). The multiple oceanographic processes in the area, *e.g.* slope currents, upwelling-downwelling processes, river plumes and eddy-like structures (Charria et al., 2017; Kersalé et al., 2016; Torres et al., 2003) interact, enhancing a high primary productivity that in turn provides food resources and important foraging opportunities for marine megafauna species. However, these oceanographic processes may be altered by climate change (García-Soto et al., 2002; Miranda et al., 2013; Santos et al., 2011) leading to the potential redistribution of the species and bringing ecological consequences (Gregory et al., 2009; Macleod, 2009). In addition, the NW and northern Iberian shelf waters include important fishing grounds for a large bottom-trawling fleet (Valeiras, 2003) and an intense maritime traffic that pose threats for the marine megafauna

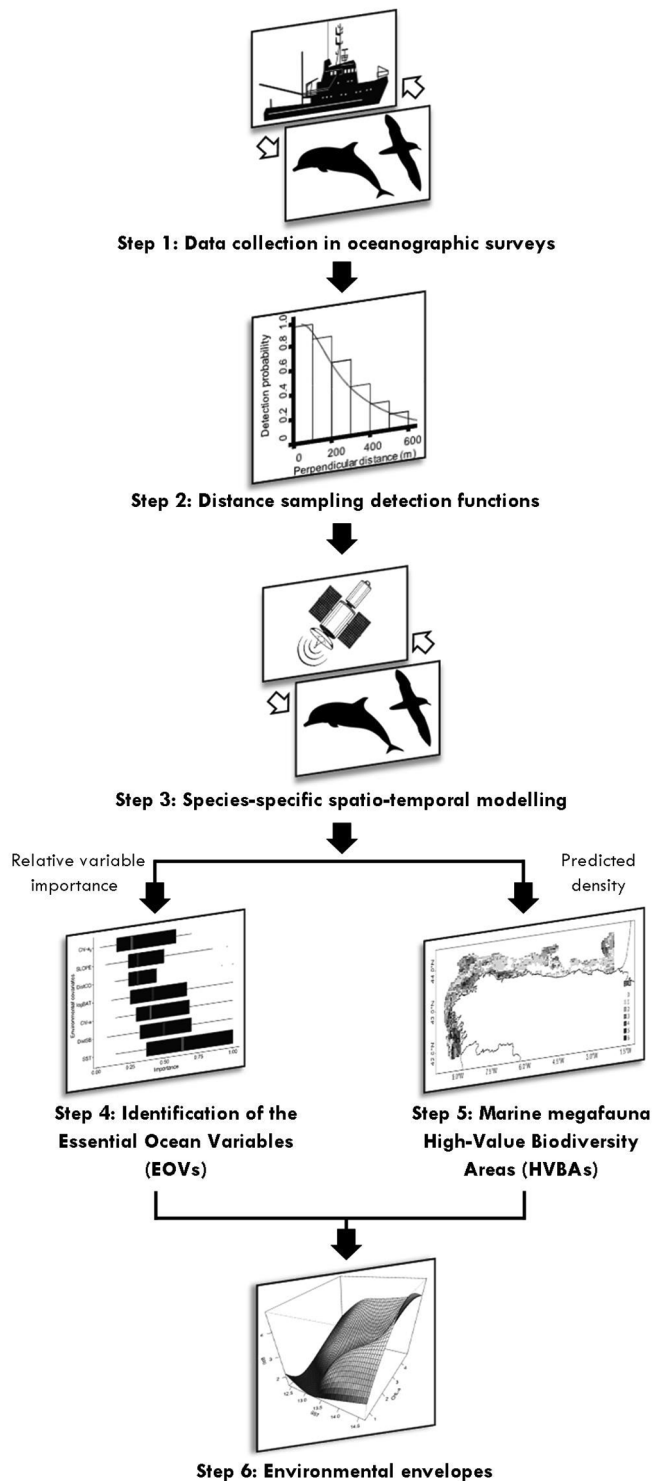


Fig. 2. Graphical representation of the methodological steps followed in this study.

community (e.g. by-catch, oil spill, vessel collision; García-Barón et al., 2019b; Pérez et al., 2010; Vieites et al., 2004). Several studies have described the oceanographic habitats of cetacean and seabird species along the French waters of the Bay of Biscay (Authier et al., 2018; Lambert et al., 2018, Lambert et al., 2017a; Laran et al., 2017; Pettex et al., 2017). However, few studies have been carried out in the NW and northern Iberian shelf waters at the megafauna community level (but Arcos et al., 2009; Louzao et al., 2019b), none of them have characterised the marine megafauna HVBAs despite the importance of this

area for the seabird and cetacean community.

This work aims to better characterise the spatio-temporal trends of the marine megafauna community (i.e. seabirds and cetaceans) of the NW and northern Iberian shelf waters in relation to ecosystem dynamics over the spring period of the last decade (2007–2016). We used a threefold approach: (i) a spatio-temporal modelling of megafauna spatial density, (ii) an identification of HVBAs and, finally, (iii) the characterisation of the environmental envelope driving megafauna diversity in our study area. Our results can serve as a first step to identify ecologically meaningful areas in the NW and northern Iberian shelf waters at the marine megafauna community level, providing the knowledge needed to support management decisions and conservation measures in a marine spatial planning context.

2. Material and methods

2.1. Data collection

Since 2007, the Spanish Institute of Oceanography (IEO) has included a standardised observer programme for marine megafauna data collection in the multidisciplinary PELACUS oceanographic acoustic survey. The PELACUS survey lasts one month and takes place annually in spring (March–April) with the aim of acoustically assessing the pelagic fish biomass along the north and NW Spanish continental shelf waters, covering an area of $\approx 42800 \text{ km}^2$ (Fig. 1). As part of the survey, marine megafauna sightings are collected following the line transect methodology (Buckland et al., 2001).

At-sea observations were collected during the period 2007–2012 on board the *R/V Thalassa* (TH) and from 2013 to 2016 on board the *R/V Miguel Oliver* (MO). The sampling protocol consisted on equidistant parallel transects perpendicular to the coastline and separated by 8 nautical miles. Data on megafauna sightings were collected by a team of three trained observers working in turns of two and placed on the highest accessible point of the vessel. This height corresponded approximately to 16 m and 12 m on the TH and MO, respectively. Observers scanned a 180° sector ahead of the vessel (from 270° to 10° on the port side and from 350° to 90° on the starboard side). Observers searched with naked eyes, and binoculars (10x42) were only used to aid species identification and to record the group size and/or animals' behaviour (Saavedra et al., 2018). Observers collected data along transects while the vessel is navigating at constant heading and speed (≈ 10 knots) during daytime. Navigation routes between predefined transect that follow a fixed course and constant 10 knots speed were also sampled when possible. Observation effort was georeferenced every minute with the vessel GPS. Surveyed transects were split into observation periods of identical detection conditions (*legs*). For each *leg*, observers recorded data on vessel speed, heading, Beaufort sea state, swell height and direction, wind speed and direction, cloud coverage, visibility, sun glare on each side of the vessel (port or starboard) and an overall subjective assessment of the detection conditions of the sightings (good, moderate or bad). For each sighting, observers recorded the time, the species, the group size, the detection distance using a stick based on the Heinemann (1981) method and its angle with respect to the track line using an angle meter. Additional data recorded for each sighting included the animal heading relative to the ship, the behaviour and the age of the individuals (presence of calves in the case of cetaceans and age-groups, if possible, in the case of seabirds, i.e. juveniles/adults based on plumage). A schematic workflow of the entire analytical process is described in Fig. 2.

2.2. Species detectability based on environmental conditions

We explored the detectability of the species based on the effect of environmental conditions by modelling the detection function to obtain the effective strip half width (ESW). Detection functions were estimated independently for each species pooling together the sightings from ten

years (2007–2016). Only sightings with swell height ≤ 2 m, Beaufort Sea-state ≤ 5 and overall medium and good visibility conditions were used following the García-Barón et al. (2019) approach. To avoid overestimation of the density, sightings of individuals attracted to the ship or associated with human activities (i.e. individuals following the R/V or scavenging on fishing discards) were systematically excluded from further analyses as Authier et al., (2018) suggested. Finally, ten seabird: Northern gannet *Morus bassanus*, Lesser black-backed *Larus fuscus*, Yellow-legged *Larus michahellis* and Mediterranean gulls *Ichthyophaga melanocephalus*, Great skua *Stercorarius skua*, Sandwich tern *Thalasseus sandvicensis*, Razorbill *Alca Torda*, Common guillemot *Uria aalge*, Balearic Puffinus *mauretanicus* and Manx shearwaters *P. puffinus* and three cetacean species: Common *Delphinus delphis* and Bottlenose dolphins *Tursiops truncatus* and Long-finned pilot whale *Globicephala melas* (Appendix A) with at least 15 sightings over the study period were included in the analysis (Authier et al., 2018).

Detection functions were modelled using both Conventional and Multiple-Covariate Distance Sampling approaches (CDS and MCDS; Buckland et al., 2001; Marques et al., 2004), with the *mrd*s R-package (Laake et al., 2015) including the effect of covariates on the detection probability in the case of the MCDS. Covariates tested included Beaufort sea-state, glare intensity, categorised swell height, cloud coverage, visibility, overall detection condition, year and observation platform (i.e. R/V). Beaufort sea-state, glare intensity, cloud coverage and visibility were included raw and as categorical covariates in the analyses (Appendix B). MCDS detection functions were fitted using forward stepwise model building based on Akaike's Information Criterion (AIC) selection, as well as by inspection of Q-Q plots and Kolmogorov-Smirnov and Cramer-von Mises goodness of fit tests (Thomas et al., 2010). The initial model was fitted without any covariate (i.e. CDS). Then, univariate models were fitted with each covariate on its own (i.e. MCDS). If the addition of a covariate provided a smaller AIC score (difference > 2), models of increasing complexity were built by comparing the score obtained by the addition of each covariate to the previous best model (Mannocci et al., 2015). Then, the process was repeated with the new best model until the addition of a new covariate did not improve the AIC (Barlow et al., 2001). Final detection function selection was made on parsimony grounds (i.e. similar explicative power but less parameters; Arnold, 2010) when the two best detection functions did not show a difference in $\Delta\text{AIC} < 2$ (i.e. $\Delta\text{AIC} < 2$). After selecting the best detection function, the ESW was calculated as the perpendicular distance in which the missing detections at smaller distances were equal to the recorded detections at bigger distances. In the case of the MCDS detection functions, the ESW was calculated for each level of the covariate.

2.3. Spatio-temporal modelling of megafauna abundance

Surveyed legs were subdivided into segments of an average of 10 km of homogeneous conditions, so the variability in environmental characteristics was limited within segments (García-Barón et al., 2019a; Virgili et al., 2017). Density surface models were then obtained for the best quality data (swell height ≤ 2 m, Beaufort Sea-state ≤ 5 and overall medium and good visibility conditions). Segments with length ≤ 5 km and segments associated with a depth > 1000 m (no representative of the sampled bathymetric range) were removed from the analysis.

Environmental covariates were selected based on biological relevance and data availability (see description in Appendix C). We used four physiographic predictors: logarithm of depth (logBAT), slope (SLOPE), the closest distance to the coast (DistCO) and to the shelf-break (measured as the distance to the 200 m-isobath; DistSB); and three oceanographic predictors: sea surface temperature (SST), logarithm of chlorophyll *a* concentration (Chl-*a*) as a proxy for phytoplankton biomass and its spatial gradient (Chl-*a*_g). We estimated the Chl-*a*_g by estimating its proportional change within a surrounding

3×3 cell grid following the Louzao et al. (2009) methodology. All oceanographic predictors were calculated by averaging the values over the surveyed period each year (i.e. March-April mean value). To eliminate the effect of varying measurements scales, all variables were standardised to a mean of 0 and a standard deviation of 1 before fitting the model (Zuur et al., 2007). Prior to the analysis, we investigated the possible co-linearity between predictors by calculating the pairwise Spearman correlation coefficients (r) and the variance inflation factor (VIF; Zuur et al., 2010). None of the pairs of variables showed high correlation ($r \geq |0.7|$ and $\text{VIF} > 3$; Dormann et al., 2013; Zuur et al., 2010) and therefore, all were included in the analysis (Table C.2).

Density surface models were fitted independently for each species by applying Generalised Additive Models (GAMs) to identify the most important environmental covariates explaining the distribution of species abundance (i.e. the number of individuals per segment). We selected a negative binomial distribution and a log-link function to account for overdispersion after checking for alternative distribution families (e.g. Tweedie). We used flexible smoothing splines to model the nonlinear functional relationship between the response variable and the covariates and the logarithm of the effective sampled area as an offset. The effective sampled area associated to each segment was calculated as the length of the segment multiplied by twice the corresponding ESW for each species.

GAMs were implemented following the Information-Theoretic framework to evaluate the competing models by assessing their relative support based on the AIC value corrected for small sample sizes (AICc) and Akaike weight (ω_i) (Burnham and Anderson, 2002). Models were constructed with all possible combinations of covariates and ranked based on their AICc. When the ω_i of the model with the lowest AICc was below 0.90, a model averaging procedure was used to account for all models and parameters' uncertainty (Burnham and Anderson, 2002). To obtain averaged coefficients and variance estimator, we identified the 95% confidence set of models where the cumulative sum of ω_i was ≥ 0.95 , starting with the model with the highest ω_i (Johnson and Omland, 2004). The ω_i were used for the assessment of the relative importance of predictor variables (Burnham and Anderson, 2002) and the response plots of the explanatory variables were constructed based on averaged coefficient of the 95% confidence set. Finally, we calculated the spatial-density predictions for each species and year on a $0.04^\circ \times 0.04^\circ$ resolution grid of covariates using the obtained averaged model. This procedure provides maps of the relative density per year for each species analysed. GAMs were conducted in R version 3.4.4 (R Core Team, 2019) using the *mgcv* R-package (Wood, 2011) with additional functions provided by the R-package *MuMIn* (functions *dredge* and *model.avg*; Barton, 2016). To validate the models, we compared the observed encounter rate (i.e. number of individuals sighted per 100 km surveyed as a proxy of the observed abundance) and the predicted relative density for each species (predicted abundance). Both average encounter rate and the average relative densities predicted were confronted in a plot for all species and the correlation coefficient of the relationship estimated was used as a measure of the global predictive performance of GAMs.

2.4. High-value biodiversity areas

High-value biodiversity areas (HVBAs) for the studied megafauna were identified based on a biodiversity richness index (BRI) which in turn relied on the areas of highest predicted abundance. Firstly, the areas of highest predicted abundance were calculated for each species and year following the Cañadas and Vázquez (2014) methodology, also applied by García-Barón et al. (2019). The estimated abundance per cell was calculated by multiplying the predicted relative density of each cell by the cell area. Then, all cells were sorted by their estimated abundance in decreasing order classifying them by ranges of 10% of the total estimated abundance in the study area. Values $> 40\%$ were selected for each species and year to delimitate the areas of highest predicted

abundance. Secondly, we obtained the BRI as the number of species for which each cell represents the highest predicted abundance area. Finally, we identified the HVBA as the areas where the highest BRI was located. The HVBA were mapped separately for seabird and cetacean species and jointly to illustrate HVBA of the megafauna community. Hence, we obtained three layers per year and three layers for the whole study period (2007–2016).

To characterise the spatial and temporal patterns of HVBA we divided our study area into five geographical sectors based on Santos et al. (2013): south Galicia (SG), from Portugal to Cape Finisterre; North Galicia (NG) from Cape Fisterra to Cape Estaca de Bares; western Cantabrian Sea (WC) from Cape Estaca de Bares to Cape Peñas; central Cantabrian Sea (CC) from Cape Peñas to Cape Ajo; and eastern Cantabrian Sea (EC) from Cape Ajo to the eastern end of the study area (see Fig. 1b). A quantitative analysis of HVBA was performed by calculating the mean value of the BRI per sector. This analysis was conducted two-fold, by year and by group of species (*i.e.* 'Community', 'Seabirds' and 'Cetaceans', categories composed by all, only seabird and only cetacean species, respectively). To assess geographical patterns in HVBA, we used two different approaches: (1) an exploration of the differences in HVBA by sector based on dissimilarities calculated using the Bray-Curtis dissimilarity distance using the *metaMDS* function in *vegan* R-package (Oksanen et al., 2018) [we assessed the differences between sectors displayed on a non-metric multidimensional scaling (nMDS) plot using the function *envfit* (*vegan* R-package) with 1000 permutations], (2) an analysis of longitudinal gradients in the HVBA by group of species fitting linear models, using the slope and r^2 . To assess temporal patterns in HVBA by sector and group of species we fitted linear models, using the slope and r^2 .

2.5. Environmental envelope of megafauna diversity

Essential Ocean Variables (EOVs) were defined by the dynamic variables that showed the highest relative predictor importance within the megafauna community (Constable et al., 2016; Lindstrom et al., 2012). At the community level, the combination of dynamic EOVs would help defining the environmental envelope (Wiens and Graham, 2005) characterising the HVBA. However, this would suggest that the underlying oceanographic conditions should differ among geographical areas, at least in relation to the variables we tested. Therefore, we calculated the averaged values of the EOVs and the BRI per year and sector to explore whether differences in EOVs could explain differences in megafauna richness. We also plotted the convex hull of the set of mean BRI values per sector. Furthermore, to describe the response of the BRI as a function of EOVs a GAM was fitted using a tensor-product smooth function of the EOVs identified and a Gaussian link function. Tensor product splines were used for n -dimensional effects, depending on the n variables considered as EOVs (Chen et al., 2012).

3. Results

3.1. Oceanographic survey data

A total of 20,942 km were surveyed over the period of ten years (2007–2016). After filtering the effort to remove those observations recorded under less optimal conditions, 15,003 km remained, representing $\approx 72\%$ of the total available effort (Table 1). Filtered survey effort ranged from a minimum of 597 km in 2013 to a maximum of 1494 km in 2007 (annual mean \pm standard deviation: 1231 ± 318 km). A total of 16,820 individuals were recorded during this period (13,730 seabirds and 3,103 cetaceans). The most common seabird species were the Northern gannet, followed by the Yellow-legged and the Lesser black-backed gulls and the Great skua, which spread throughout the study area (see figures in Appendix A). The Razorbill, the Sandwich tern, the Mediterranean gull and the Balearic shearwater were observed mainly over the western and south-western

Table 1

Total effort, effort on good visibility conditions (Beaufort sea-state ≤ 5 , swell height ≤ 2 m and medium to good general conditions), effort after removing segments of length ≤ 5 km, effort after removing segments with a depth > 1000 m and number of segments for each year of the PELACUS survey.

Year	Effort (km)	Filtering visibility conditions (km)	Filtering segments ≤ 5 km (km)	Filtering depth > 1000 m (km)	Number of segments
2007	1695.91	1608.62	1522.95	1494.61	150
2008	2250.15	1506.56	1429.26	1387.16	145
2009	2908.02	2665.37	1786.83	1716.17	189
2010	3286.61	1784.68	977.26	903.29	98
2011	1338.21	1198.50	1153.20	1153.20	121
2012	2063.06	1124.70	1087.53	1087.54	108
2013	1835.80	1036.57	597.93	597.94	61
2014	1836.52	1387.51	1428.43	1397.24	145
2015	1857.08	1427.00	1367.69	1367.69	141
2016	1871.11	1263.52	1217.14	1207.52	130
Total	20942.47	15003.03	12583.24	12312.36	1288

sector of the study area. The less frequent species were the Common guillemot, sighted sparsely over the study area and the Manx shearwater for which the sightings were mainly concentrated over the western sector. The most common cetacean species were the Common and the Bottlenose dolphins, followed by the Long-finned pilot whale. These three species were recorded over the whole study area, with the Common dolphin found especially over the western sector and the Bottlenose dolphin encountered mainly over the eastern sector (see figures in Appendix A).

3.2. Species detectability

Detections functions were estimated based on the sightings that remained after filtering for weather conditions. The best model for four species did not include any covariate (CDS) and included at least one covariate for nine species (MCDS) (Table 2). In MCDS models, the most selected covariates were visibility ($n = 4$) and Beaufort sea-state ($n = 4$) either raw or categorised, followed by swell height ($n = 3$), year ($n = 1$) and general conditions ($n = 1$). The average ESW was 240 m (CV = 0.36) for seabird species and 550 m (CV = 0.34) for cetacean species (Table 2).

3.3. Spatio-temporal modelling of marine megafauna

After filtering the effort and excluding segments of ≤ 5 km and segments with a depth > 1000 m, a total of 1288 segments were used to fit the density surface models (see Table 1; Appendix D). The number of models combined to achieve the 95% confidence set ranged from 4 to 78 out of a total of 98. The most important covariates (*i.e.* environmental covariates with importance $> 50\%$ for at least 5 species) describing the spatial abundances of the species were SST ($n = 7$), DistSB ($n = 5$), Chl-a ($n = 5$) and logBAT ($n = 5$) (Fig. 3 and D.1). Those covariates that appeared in all the species-specific models combined to achieve the 95% confidence set (*i.e.* 100% importance) were SST ($n = 4$), DistSB ($n = 2$), Chl-a ($n = 1$), logBAT ($n = 1$) and DistCO ($n = 2$). For seabird species, the most important covariates describing their spatial abundance were SST, DistSB, logBAT and Chl-a, whilst in the case of cetaceans the main covariates were SST, Chl-a, SLOPE and DistSB (Fig. D.1). The Yellow-legged gull, the Razorbill, the Manx and the Balearic shearwater showed preference for a strictly coastal habitat, whilst the Lesser black-backed gull, the Mediterranean gull and the Great skua showed preference for shelf and slope areas. Other species, such as the Sandwich tern, the Common guillemot, the Northern gannet and the Common dolphin were classified as ubiquitous as they were widely sighted over the whole study area. The Bottlenose dolphin and

Table 2
Results of the best fitted detection functions for each species: Sightings (number of sightings used to fit the detection function); Model (type of model used to fit the detection function, MCDS: Multi Covariate Distance Sampling or CDS: Conventional Distance Sampling); Key (type of detection function, hr: hazard-rate or hn: half-normal); Detection covariate (environmental covariates used to fit the detection function), w (m) (truncation distance in meters); Pa (averaged detection probability); SE Pa (standard error of the detection probability); ESW (effective strip half-width for CDS models and averaged effective strip half-width for MCDS models obtained from the detection function) and CV ESW (coefficient of variation of the ESW in the case of MCDS).

Family	Species	Scientific name	Code	Sightings	Model	Key	Covariate	w (m)	Pa	SE Pa	ESW (m)	CV ESW
Seabird	Sulidae	Northern gannet	MORBAS	6440	MCDS	hr	visibility categorized general conditions	1000	0.37	0.01	380	0.21
	Laridae	Lesser black-backed gull	LARFUS	1213	MCDS	hr	visibility year	1000	0.20	0.007	325	0.74
Stercorariidae	Yellow-legged gull	<i>Larus michahellis</i>	LARMIC	1626	MCDS	hr	visibility	500	0.29	0.02	180	0.33
		<i>Ichthyophaga melanocephalus</i>	IGHMEL	45	MCDS	hn	visibility	500	0.53	0.08	340	0.37
	Great skua	<i>Stercorarius skua</i>	STESKU	334	MCDS	hr	Beaufort	600	0.41	0.04	275	0.19
		<i>Thalasseus sandvicensis</i>	THASAN	118	MCDS	hr	swell height categorized	800	0.20	0.05	200	0.34
Sternidae	Sandwich tern	<i>Alca torda</i>	ALCTOR	128	CDS	hr	Beaufort categorized	500	0.36	0.03	180	-
	Razorbill	<i>Uria aalge</i>	URIAAL	78	CDS	hr		300	0.35	0.09	110	-
Procellariidae	Balearic shearwater	<i>Puffinus mauretanicus</i>	PUFMAU	96	MCDS	hn	visibility categorized	500	0.44	0.04	230	0.18
		<i>Puffinus puffinus</i>	PUFPUF	66	CDS	hn		350	0.50	0.04	180	-
	Manx shearwater	<i>Delphinus delphis</i>	DELDEL	74	CDS	hr		1000	0.34	0.07	340	-
Delphinidae	Common dolphin	<i>Tursiops truncatus</i>	TURTRU	93	MCDS	hn	Beaufort categorized	1300	0.40	0.07	700	0.34
	Bottlenose dolphin	<i>Globicephala melas</i>	GLOMEL	69	MCDS	hn	swell height categorized	1500	0.30	0.07	620	0.13
Cetacean	Long-finned pilot whale	<i>Globicephala melas</i>	GLOMEL	69	MCDS	hn	Beaufort categorized	1500	0.30	0.07	620	0.13

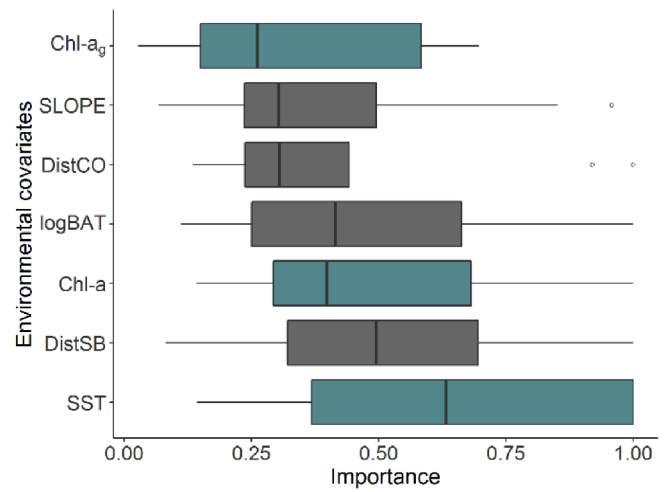


Fig. 3. Boxplot of the relative importance of the variables considered for the seabird and cetacean community. Dynamic variables (in green): sea surface temperature (SST), logarithm of chlorophyll-a concentration (Chl-a) and its spatial gradient (Chl-a_g) and static variables (in grey): the closest distance to the shelf-break (DistSB), the closest distance to the coast (DistCO), slope (SLOPE) and logarithm of depth (logBAT).

the Long-finned pilot whale were associated with the slope. Globally, the predictive power of our models was high given the high correlation with the observed relative density based on the encounter rate (p-value < 0.001, $r^2 = 0.712$; Fig. D.2).

3.4. High-value biodiversity areas

We identified the HVBA based on the BRI calculated from the highest 40% of the species predicted abundance (Appendix E). For cetaceans, the HVBA (BRI = 3, i.e. all the cetacean species analysed) were located over the western and NW shelf break, Avilés and Capbreton canyons (Fig. E.1). In the case of seabirds, the HVBA were located over the Rías Baixas, NW coast, Ferrol canyon, the Masma Gulf, El Cachucho and Landes Plateau. The seabirds' HVBA with the maximum value of BRI (BRI = 7, i.e. 70% of the seabird species analysed) was located over the Rías Baixas (Fig. E.2). In relation to the megafauna community (i.e. cetacean and seabird species), the HVBA with the maximum value of BRI (BRI = 8, i.e. 61% of the species analysed) were located over the Rías Baixas and the western and NW shelf break (Fig. E.3). Results of the linear models showed that the HVBA were stable over the study period (Fig. E.4): the main habitats for cetaceans were located in the western and NW shelf break (Fig. 4a), whilst seabirds were mainly concentrated on the Rías Baixas and the Ártabro and Masma Gulfs (Fig. 4b). The HVBA of the whole community were located over the western and NW Spanish waters and the Masma Gulf (Fig. 4c).

3.5. Environmental envelope

The nMDS plot performed for the assessment of the geographical patterns of HVBA (Fig. E.5) showed three well differentiated groupings: (1) the sectors located on the eastern part of the study area, EC and CC; (2) the WC and NG sectors, located on the centre and the NW part of the study area; and (c) the SG sector, located on the south-western part of the study area. Results of the linear models showed a negative slope in the case of the whole marine megafauna community and the seabird community, indicating that HVBA decreased from the SG towards the EC. In the case of the cetacean community, the linear models showed a slope close to 0 indicating that HVBA were distributed over the whole study area (Fig. E.5).

We defined the SST and the Chl-a as dynamic EOVs for the

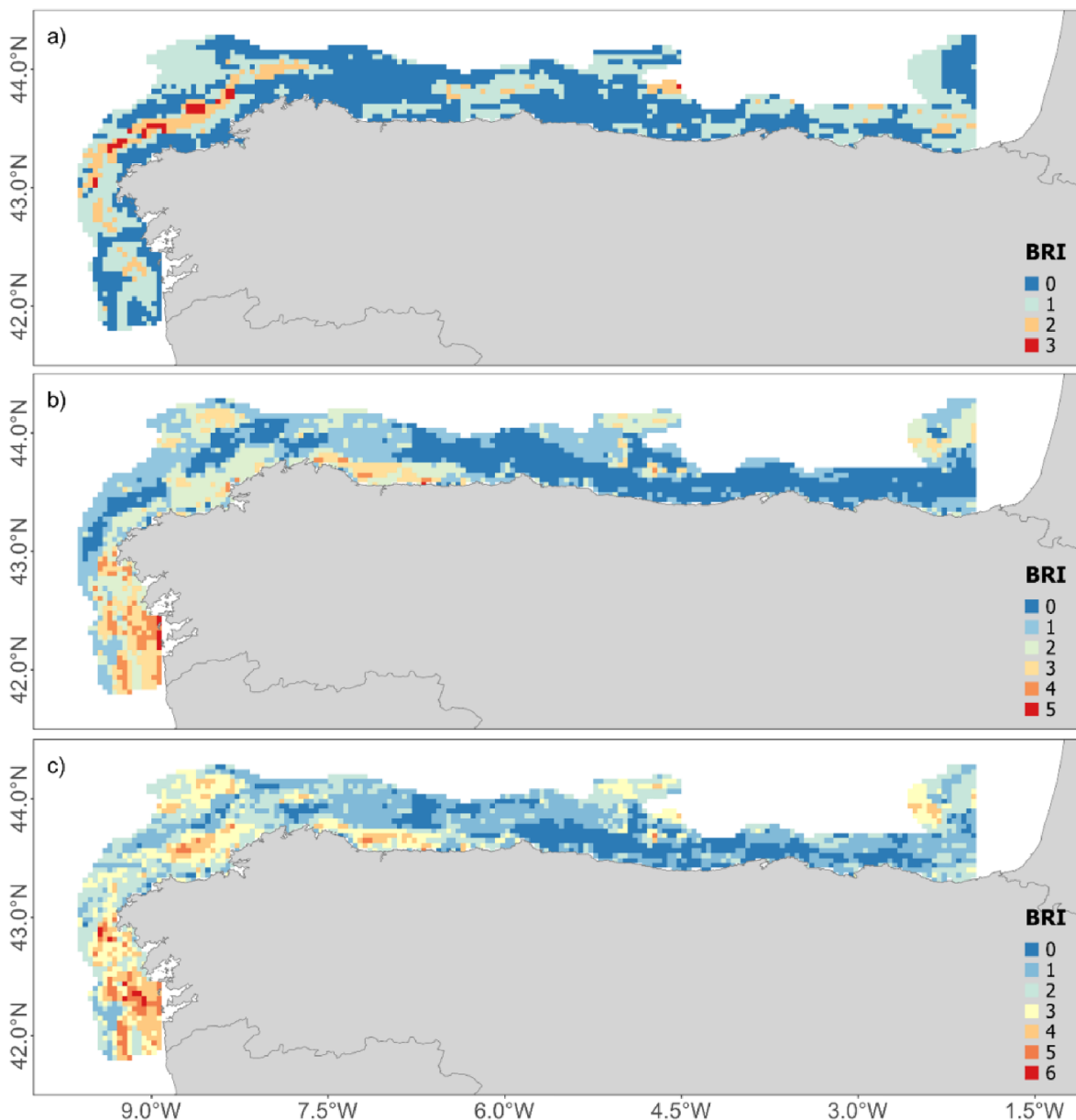


Fig. 4. Maps showing the high-value biodiversity areas based on the mean biodiversity richness index (BRI) from the time-series 2007–2016 for a) cetaceans, b) seabirds and c) the megafauna community (seabirds and cetaceans).

megafauna community, as they showed the highest relative importance (> 50%) for at least 5 modelled species. Thus, plotting the mean BRI per sector and year as a function of the SST and Chl-a gave us an overall pattern (see Fig. 5a) showing that higher SST and Chl-a values corresponded to higher mean BRI. The highest values of mean BRI shaped the convex hull of the SG sector. The other four sectors (NG, WC, EC and CC) and their respective convex hulls revealed similar patterns and were located together, but separately from the SG sector. These four sectors showed less variability in the SST and Chl-a values among years; thus, their convex hulls were smaller than the convex hull defined by the SG sector.

Finally, the GAM fitted to describe the response of the BRI as a function of the EOVs explained 72.3% of the deviance (approximate significance of smooth terms: edf = 10.8 and p-value < 0.001; AIC 42.5 units lower than the null model). The 3D smoothers obtained (Fig. 5b) showed that maximum BRI corresponded to higher SST and Chl-a values, whilst the BRI was lower at mean values of SST and Chl-a.

4. Discussion

The NW and northern Iberian waters are transition waters located between the boreal and subtropical environments, being a diversity hotspot area for multiple species with different biogeographic ranges (Andonegi et al., 2015; Valdés et al., 2002). Capitalising on the PELACUS spring survey, we integrated data of ten seabird species (ranging from the smaller Manx shearwater to the larger Northern gannet) and three cetacean species (the Common dolphin, the Bottlenose dolphin and the Long-finned pilot whale) that constitute the spring megafauna community of the northern and NW Iberian waters. We described the spatial and temporal changes of their HVBA and identified the EOVs shaping their environmental envelope during early spring. This is one of the first studies that develop a community level approach in this area, with other long-term studies documenting the relative abundance changes of top predators over time (Authier et al., 2018) or describing their species-specific habitat preferences (Díaz López and Methion, 2019; Lambert et al., 2018).

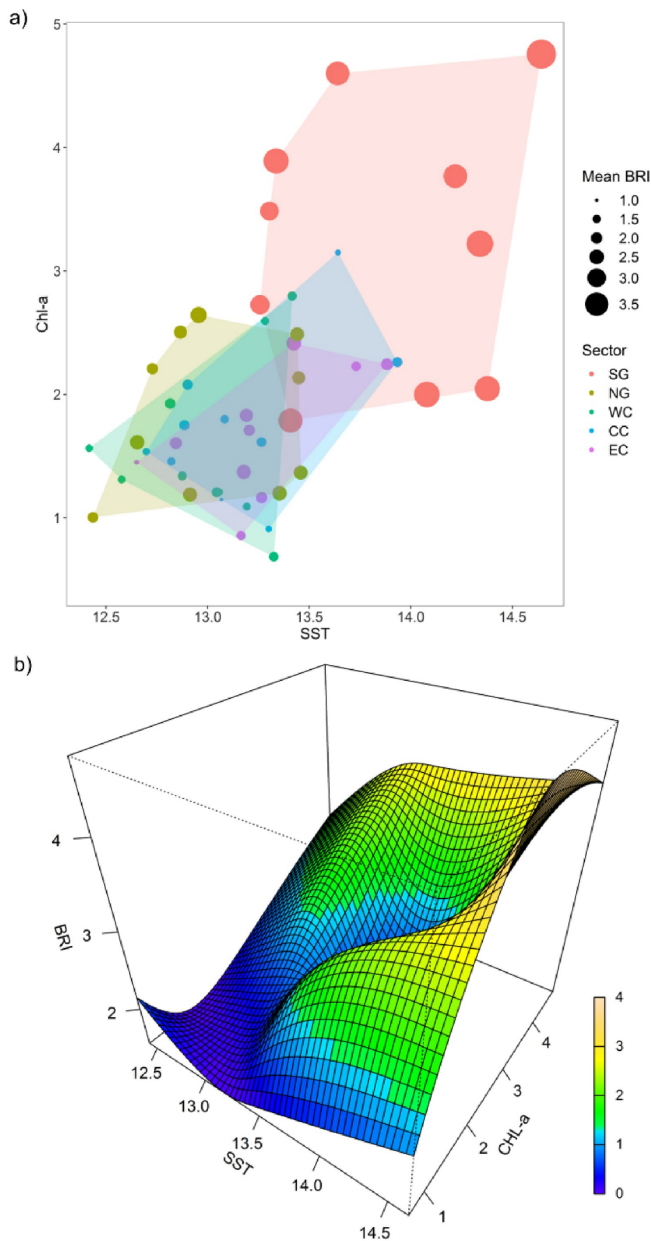


Fig. 5. Environmental envelope showing: a) mean biodiversity richness index (BRI) per sector and year according to the averaged values of sea surface temperature (SST) and logarithm of chlorophyll-a concentration (Chl-a) per sector and year and b) three-dimensional Generalized Additive Model graphic output with the BRI as a function of SST and Chl-a. Sector references are located in Fig. 1b.

Notwithstanding that the density estimates should be considered as relative (we have not formally corrected for availability and perception bias) and our data cover only the spring period, our estimates can still reflect the general spatial patterns of the marine megafauna community abundance over the study area and can contribute to inform about their HVBA and environmental envelopes. Furthermore, even though our data were collected only in spring, it has the value of being a long-term (*i.e.* 10 years) series, allowing the interpretation of annual changes, something not possible at present on the basis of dedicated seabird and cetacean surveys, that tend to have a decadal periodicity (*e.g.* SCANS surveys; Hammond et al., 2017). Thus, this paper shows the need for integrating individual species data to locate areas of community-level importance for the marine megafauna and evidences the value of annual integrated oceanographic surveys (Doray et al., 2018).

4.1. Environmental envelopes

Defining EOVs for a community implies identifying the most important overall predictors of distribution and abundance of the species which form that community. In our case, both physiographic and oceanographic descriptors were important drivers of the distribution patterns of the species considered. Specifically, the SST and the Chl-a concentration were the most important dynamic descriptors, while the distance to the shelf break was the most important physiographic descriptor. The importance of SST and Chl-a driving marine ecosystem functioning can be explained because they indicate the provision of nutrient-rich deep waters to the surface (*i.e.* upwelling systems), planktonic productivity and phytoplankton blooms (Bode et al., 2009; Friedland et al., 2012). Variation in the SST and the Chl-a concentration are likely associated with prey retention, highlighting dense prey patches available to predators (Yen et al., 2004). Thus, these EOVs can shape the marine ecosystem from plankton, to mid-trophic level fish, up to apex predators such as seabirds and cetaceans (Lehodey et al., 2010). The response of the organisms to these EOVs differs across trophic levels, whilst lower-trophic levels (plankton) may be directly influenced by the SST and the Chl-a concentration, mid- and upper-trophic levels (from small pelagic fishes to apex predators) may respond to changes in prey caused by changes in the EOVs. Hence, the SST and the Chl-a concentration were highlighted as EOVs in line with results from other studies which have shown their importance in driving the large-scale patterns of marine megafauna (Grémillet et al., 2008; Whitehead et al., 2008).

Overall, marine megafauna abundance was positively influenced by both dynamic descriptors, which define the environmental envelope shaping areas of higher density. Thus, HVBA were associated with higher values of SST and Chl-a concentration shaping the specific environmental envelope for the study period. These HVBA were mainly located in the western and NW area (SG and NG sectors) and decreased towards the inner Bay of Biscay (from SG to EC sectors). The waters of the SG sector are highly productive due to a large phytoplankton bloom that develops over the shelf between March–April, starting gradually in coastal waters and progressively extending to the outer shelf and oceanic regions (Bode et al., 2003; Figueiras et al., 2002) caused by persistent northerly wind forcing. In addition, the strongest rivers runoffs that transport inland nutrients further offshore coincide with the onset of these northerly winds (Picado et al., 2016; Teles-Machado et al., 2016), increasing the Chl-a concentration over the area and creating a highly attractive and temporally stable oceanographic feature. In fact, these areas showed a highly diverse marine megafauna community over our study period and consistent HVBA. They may indicate areas of persistent oceanographic features which enhance productivity attracting in turn elevated numbers of marine megafauna species (Bouchet et al., 2015). Although upwelling areas are characterised by colder waters, the SST values of our study period (March–April) reached the highest values in the SG sector and decreased towards the eastern Bay of Biscay (WC, CC and EC sectors). This phenomenon may be explained by the influence of the “Navidad” current, a prolongation of the poleward current, which inflows into the Bay of Biscay around Cape Fisterra supplying warm waters along the NW shelf and slope. The influence of the “Navidad” current is evident until April (Pingree, 1994; Sánchez and Gil, 2000; Torres et al., 2003).

Secondly, HVBA also extended into the NG sector over the shelf-break. This result is in line with previous studies which indicated that continental shelf-breaks appear to be highly productive habitats, which frequently support high densities of marine predators (Certain et al., 2008; Lambert et al., 2017a). Due to the site-specific oceanographic features over these areas, zooplankton often aggregates close to the surface making prey available to diving predators (Certain et al., 2008; Croll et al., 1998). Both, the SG and NG sectors showed higher values of biodiversity overlapping with the fishing grounds of a large bottom-trawling fleet operating in the shelf and upper slopes (Valeiras, 2003).

Seabirds and cetaceans foraging in the study area show a diverse diet comprising pelagic and demersal prey, most of them also of commercial interest, such as the European sardine *Sardina pilchardus* [e.g. the Balearic shearwater (Meier et al., 2016; Navarro et al., 2009), the Great skua (Votier et al., 2007), the Northern gannet (Hamer et al., 2007; Lewis et al., 2003), the Yellow-legged and the Lesser black-backed gulls (Alonso et al., 2015; Calado et al., 2018), the Common and the Bottlenose dolphin (Santos et al., 2013; Spitz et al., 2006)], the Blue whiting *Micromesistius poutassou* [e.g. the Balearic and the Manx shearwaters (Gray and Hamer, 2001; Navarro et al., 2009), the Northern gannet (Hamer et al., 2007), the Great skua (Käkelä et al., 2006), the Yellow-legged gull (Alonso et al., 2015), the Common and the Bottlenose dolphin (Meynier et al., 2008; Spitz et al., 2006) or the Horse mackerel *Trachurus trachurus* [e.g. the Balearic shearwater (Meier et al., 2016), the Yellow-legged and the Lesser black-backed gulls (Calado et al., 2018; Kubetzki and Garthe, 2003), the Northern gannet (Hamer et al., 2007)]. Furthermore, this fishing activity provides also food for many of these species in the form of fishery discards (Depestele et al., 2016; Díaz López et al., 2019; Valeiras, 2003; Louzao et al., 2020b).

HVBAs were stable over the time-series, both for seabird and cetacean species, showing the importance of the western and NW area (SG and NG sectors) for the marine megafauna community during early spring. As other studies in the area have demonstrated (Arcos et al., 2009; Louzao et al., 2019b), this result highlights the niche persistence of the marine megafauna community over time. Areas of high biodiversity capture key ecosystem functions and services, such as productivity and stable food dynamics (Dulvy et al., 2004; Palumbi et al., 2008). Thus, the spatial stability of the HVBAs can be used to define areas of conservation importance which we argue is essential for the identification of conservation management measures. Furthermore the HVBAs identified overlap with the eight IBAs (Important Birds Areas) identified over the northern and NW Iberian continental shelf during early autumn (Arcos et al., 2009). This shows that HVBAs may be year-round important areas for the marine megafauna community, supporting the designation of these marine protected areas as part of the Natura 2000 network.

4.2. Implications of the EOVs for the conservation of the HVBAs

The underlying relationship between EOVs and specific biological communities justifies the long-term monitoring of EOVs (Constable et al., 2016). Analysis of temporal and spatial variability in EOVs could help identify areas of persistent dynamic oceanographic features (Louzao et al., 2012) that create relatively stable habitat associations of upper-trophic marine predators and serve to locate HVBAs (Lambert et al., 2018). Monitoring EOVs could therefore support spatially dynamic ocean management (Hobday et al., 2014).

An additional advantage of EOv monitoring would be the detection of changes resulting from specific anthropogenic pressures (Constable et al., 2016) or the forecasting of the response of the species or communities in the face of climate change. As noted before, the location of the primary HVBAs matches with the area which has the highest number of fishing vessels (≈ 4200 to date; <https://www.pescadegalicia.gal/rexboque/>) and where the highest amount of their catches is landed, making the area one of the main fishing regions at European and worldwide scales (Vázquez-Rowe et al., 2011). Most of the fishing gears used in this area, such as pelagic or bottom trawl nets, gillnets or longlines, pose a risk of bycatch for large marine vertebrates, such as seabirds and cetaceans (Díaz López et al., 2019; Goetz et al., 2015; Rodríguez et al., 2013; Saavedra et al., 2018). HVBAs could help identify areas with the highest risk of interaction with fisheries guiding where to concentrate management and conservation efforts especially aimed at marine megafauna. Management measures could include the spatio-temporal controlling of fishing effort through seasonal fishery exclusion zones, mandatory monitoring or enforcement of bycatch

mitigation measures (Dudley et al., 2012; Løkkeborg, 2003).

This study provides an example of the monitoring of EOVs and the identification of HVBAs. It highlights the importance of long-term monitoring to measure changes through time, assisting scientists, managers and policy makers to forecast and prepare for a possible redistribution of species due to climate change or other pressures, with ecological, social and economic consequences (Miloslavich et al., 2018). In addition, the identification of HVBAs is crucial to identify where conservation efforts are required, to assist with the allocation of resources (García-Barón et al., 2019; Lambert et al., 2017b). HVBAs may help to identify new potential marine protected areas or quantify gaps in the current network of protected areas (e.g. Natura 2000 network). This is particularly important in the context of climate change, where quantitative and spatial changes in HVBAs may indicate a reorganization of the marine megafauna community and potential shifts of vertebrate biomass (Sydemann et al., 2015) into areas lacking conservation measures. Our results provide valuable information for the ecological system of the NW and northern Iberian waters to detect changes and anticipate their consequences. Under the current scenario of ecosystem reorganization due to climate change (Gregory et al., 2009; Hemery et al., 2007; Macleod, 2009), maintenance and appropriate funding for the large scale long-term monitoring programmes of the marine ecosystem continues to be essential. In addition, these type of studies are important to fulfil the emergent need of sound spatial information to support marine spatial planning approaches and are needed to improve the management and conservation of the marine megafauna species and/or communities at their key areas (IPBES, 2019).

CRedit authorship contribution statement

Isabel García-Barón: Conceptualization, Methodology, Formal analysis, Visualization, Investigation, Writing - original draft, Writing - review & editing. **M. Begoña Santos:** Conceptualization, Supervision, Writing - review & editing. **Camilo Saavedra:** Resources, Writing - review & editing. **Amaia Astarloa:** Resources. **Julio Valeiras:** Resources. **Salvador García Barcelona:** Resources. **Maite Louzao:** Conceptualization, Supervision, Writing - review & editing.

Declaration of Competing Interest

The authors declare that they have no known competing financial interests or personal relationships that could have appeared to influence the work reported in this paper.

Acknowledgments

Thanks to PELACUS (IEO) crew and scientists for all their support during oceanographic surveys, especially to marine predator observers. We also thank Anna Rubio and Yolanda Sagarminaga for their helpful suggestions. I.G-B. was funded by a PhD fellowship from the Spanish Government (BES-2014-070597) and C.S. by a PhD fellowship from the Spanish Institute of Oceanography (BOE-A-2011-2541). M.L. was funded by a Ramón y Cajal (RYC-2012-09897) contract from the Spanish Government. This study is a contribution to the CHALLENGES project (CTM2013-47032-R). The contribution number is 964 from AZTI (Marine Research).

Appendix A. Supplementary data

Supplementary data to this article can be found online at <https://doi.org/10.1016/j.ecolind.2020.106504>.

- Virgili, A., Lambert, C., Pettex, E., Dorémus, G., Van Canneyt, O., Ridoux, V., 2017. Predicting seasonal variations in coastal seabird habitats in the English Channel and the Bay of Biscay. *Deep. Res. Part II Top. Stud. Oceanogr.* 141, 212–223. <https://doi.org/10.1016/j.dsr2.2017.03.017>.
- Votier, S.C., Bearhop, S., Crane, J.E., Manuel Arcos, J., Furness, R.W., 2007. Seabird predation by great skuas *Stercorarius skua* - Intra-specific competition for food? *J. Avian Biol.* 38, 234–246. <https://doi.org/10.1111/j.0908-8857.2007.03893.x>.
- Whitehead, H., McGill, B., Worm, B., 2008. Diversity of deep-water cetaceans in relation to temperature: Implications for ocean warming. *Ecol. Lett.* 11, 1198–1207. <https://doi.org/10.1111/j.1461-0248.2008.01234.x>.
- Wiens, J.J., Graham, C.H., 2005. Niche Conservatism: Integrating Evolution, Ecology, and Conservation Biology. *Annu. Rev. Ecol. Evol. Syst.* 36, 519–539. <https://doi.org/10.1007/s00408-009-9147-5>.
- Wood, S.N., 2011. Fast stable restricted maximum likelihood and marginal likelihood estimation of semiparametric generalized linear models. *J. R. Stat. Soc. Ser. B (Statistical Methodol.)* 73, 3–36.
- Yen, P.P.W., Sydeman, W.J., Hyrenbach, K.D., 2004. Marine bird and cetacean associations with bathymetric habitats and shallow-water topographies: Implications for trophic transfer and conservation. *J. Mar. Syst.* 50, 79–99. <https://doi.org/10.1016/j.jmarsys.2003.09.015>.
- Zuur, A.F., Ieno, E.N., Elphick, C.S., 2010. A protocol for data exploration to avoid common statistical problems. *Methods Ecol. Evol.* 1, 3–14. <https://doi.org/10.1111/j.2041-210X.2009.00001.x>.
- Zuur, A.F., Ieno, E.N., Smith, G.M., 2007. *Analysing Ecological Data*. Springer, New York. <https://doi.org/10.1016/B978-0-12-387667-6.00013-0>.